

Oxic microzones and radial oxygen loss from roots of *Zostera marina*

Sheila Ingemann Jensen¹, Michael Kühl^{1,*}, Ronnie Nøhr Glud¹,
Lise Bolt Jørgensen², Anders Priemé³

¹Marine Biological Laboratory, Institute of Biology, University of Copenhagen, Strandpromenaden 5, 3000 Helsingør, Denmark

²Department of Evolutionary Biology, Institute of Biology, University of Copenhagen, Gothersgade 140, 1123 Copenhagen K, Denmark

³Department of Microbiology, Institute of Biology, University of Copenhagen, Sølvgade 83H, 1307 Copenhagen K, Denmark

ABSTRACT: Oxygen microelectrodes and planar oxygen optodes were used to map the microdistribution of oxygen and the radial oxygen loss (ROL) from roots of *Zostera marina* kept in natural sediment. Substantial heterogeneity in the oxygen distribution was seen along the roots, with oxygen mainly leaking out from the root tips. Maximum oxygen levels at the root surface reached 19 to 80 % of air saturation in the light and the oxygenated zone extended 1 to 2 mm away from the root tip. The oxygen concentration at the root surface decreased to 0–5 % of air saturation at positions 3 to 6 mm behind the root apex. The high oxygen levels at the root tip surface were due to an effective barrier to ROL on the older part of the roots and the presence of an effective gas-transport system in the plant, with numerous intercellular spaces extending very close to the apical meristem of the root. Radial diffusion of oxygen from the root surface created a dynamic 0 to 1 mm-wide oxic microzone around the ~0.3 mm wide roots of *Z. marina* that varied with irradiance and distance from the root tip. Root-surface oxygen concentrations and ROL measured 2 mm behind the apex increased with increasing irradiance until ROL saturation was reached at irradiances >400 $\mu\text{mol photons m}^{-2} \text{s}^{-1}$. The ROL increased from 16.2 $\text{nmol O}_2 \text{cm}^{-2} \text{h}^{-1}$ in darkness to 21.6, 28.8 and 36.0 $\text{nmol O}_2 \text{cm}^{-2} \text{h}^{-1}$ at incident irradiances of 25, 111 and 467 $\mu\text{mol photons m}^{-2} \text{s}^{-1}$, respectively. Based on measured steady-state radial oxygen profiles, the total oxygen export from one 6 cm long root of the first actively growing root bundle with a total surface area of 0.56 cm^2 was estimated to be 6.0 to 6.7 $\text{nmol O}_2 \text{h}^{-1}$ in saturating light. The total subsurface input of plant-mediated oxygen was estimated to be only in the order of 2 to 14 % of the total diffusive oxygen uptake (DOU) across the sediment–water interface. The local input of oxygen from the root tip was, however, similar to the DOU at the primary sediment–water interface, and 35 to 43 % of the total oxygen loss occurred from the outermost 0 to 3.5 mm of the root tip. The roots of *Z. marina* grow ~5 mm d^{-1} , and significant oxygen levels will therefore only be present at a given spot for less than 24 h during root growth. The rhizosphere of *Z. marina* is thus characterised by a constantly changing mosaic of ephemeral oxic microniches in the reduced sulphidic sediment, leaving behind an anoxic but oxidised zone around the more mature parts of the roots.

KEY WORDS: Radial oxygen loss · Microelectrodes · Optodes · *Zostera marina* · Rhizosphere

Resale or republication not permitted without written consent of the publisher

INTRODUCTION

The radial oxygen loss (ROL) from the roots of submerged plants growing in anoxic sediments may increase the oxic–anoxic interface significantly and may therefore have a profound effect on the zonation of the biogeochemical processes in sediments (e.g.

Terrados et al. 1999 [redox potential], Welsh et al. 2000 [nitrification], Herbert & Morse 2003 [sulphide and ferric iron]). Measurements of the total oxygen loss from aquatic plants have shown that the oxygen leakage is highly variable among different species (Sand-Jensen et al. 1982, Caffrey & Kemp 1991) and also depends on physical conditions such as temperature, water flow

*Corresponding author. Email: mkuhl@bi.ku.dk

and light. The use of platinum electrodes on plants rooted in agar showed that the ROL was variable along the root axis in different wetland species (e.g. Armstrong 1971 [*Oryza* spp.], Connell et al. 1999 [*Halophila ovalis*], Armstrong et al. 2000 [*Phragmites australis*]), with substantial ROL only occurring close to the root tips and the fine lateral roots. However, other wetland plants seem to have a more uniform ROL along the length of the roots (e.g. Christensen et al. 1994, Visser et al. 2000, Colmer 2003). A barrier to ROL is thought to be of adaptive value for plants in anaerobic environments (Armstrong 1979) by ensuring an adequate oxygen supply to the active root tips during elongation.

The barrier to ROL might also be of protective value to the plant against invasion of toxic substances, like sulphide, from the surrounding anoxic sediment (Armstrong & Armstrong 2001). Sulphate reduction is the quantitatively most important anaerobic degradation process in coastal marine sediments (Jørgensen 1982) and can generate high sulphide concentrations in reduced sediments. Sulphate reduction rates have been shown to be higher in *Zostera marina*-colonised sediments than in bare sediments of similar origin (Holmer & Nielsen 1997), and a light-induced increase in sulphate reduction rates has also been suggested as a consequence of leakage of dissolved organic carbon from the plant roots (Blaabjerg et al. 1998). Herbert & Morse (2003), however, found a major decrease in pore-water sulphide concentrations in the root zone of *Z. marina* sediments during light exposure.

Factors causing low intra-plant oxygen concentrations are thought to be a central cause for recently observed mass mortality events of (e.g.) the seagrass *Zostera marina* (Greve et al. 2003). Intra-plant oxygen concentrations are highly affected by ROL from the root system and vary with water flow (T. Binzer pers. comm.), light and temperature (Greve et al. 2003). Low intra-plant oxygen concentrations are inversely correlated with intra-plant H_2S concentrations in darkness (Pedersen et al. 2004), and the inward diffusion of toxic H_2S may thus be correlated with an inability to sustain an oxic microzone around the roots. However, a detailed study of the spatial distribution of oxygen in the rhizosphere of *Z. marina* kept in their natural substratum is still lacking.

In this study we investigated the spatial distribution of oxygen and ROL along the roots of *Zostera marina*. To quantify the possible dynamics under natural conditions we also investigated ROL from the root tip under different light regimes. To map the oxygen micro-environment around the roots in its natural substratum and to determine the extension of an oxic microshield against H_2S , we used Clark-type oxygen microsensors previously used in other investigations of ROL from

plants (e.g. Caffrey & Kemp 1991, Pedersen et al. 1998, Revsbech et al. 1999). Furthermore, first attempts to map the 2-dimensional distribution of oxygen around *Z. marina* roots with optical oxygen indicator foils (planar optodes) are presented and compared to the microelectrode approach. Planar optode measurements have previously been used to map the oxygen distributions in sediments and biofilms (e.g. Glud et al. 1996, 1999), but besides a recent application for mapping oxygen in the rhizosphere of *Spartina* spp. (Nordi 2004), this is so far the only application of planar oxygen optodes to map the heterogeneous oxygen distribution around the roots of aquatic plants. Our study presents the first detailed mapping of the microdistribution of oxygen in the rhizosphere of *Z. marina*.

MATERIALS AND METHODS

Study site. Plants, water (salinity of 15 to 20) and sediment were collected from an eelgrass bed near Rungsted Harbour, Denmark. Plant clusters of 2 to 20 plants with surrounding sediment were collected with a spade at a water depth of ~1 m, and sediment was carefully separated from the plant roots. Water, plants (immersed in water from the sampling site) and sediment were transported to the laboratory in separate containers within <1 h of sampling. In the laboratory, the plants were replanted in sieved sediment from the sampling site (mesh size 1 mm) and immersed in a large aquarium with 25 l filtered and aerated water. Plants were grown in a thermostatted room (16°C) in a 14:10 h light:dark cycle under an irradiance of 250 $\mu\text{mol photons m}^{-2} \text{s}^{-1}$ (Son-T Argo 400, Phillips) for at least 3 wk prior to the experiments. Several submersible pumps provided continuous stirring of the water. Before measurements, 1 plant was replanted in a separate plastic box containing sediment from the sampling site and placed in a 5 l aquarium positioned underneath a fibre-optic tungsten/halogen lamp (KL-2500, Schott) with the leaves centred in the light field of the lamp. Submersible pumps induced stirring of the water and air saturation of the water was ensured by a continuously flushing air pump. Downwelling irradiance was measured with a quantum irradiance meter (LiCor) immediately above the water surface for all experiments.

Microsensor measurements. Microscale oxygen measurements were made with Clark-type oxygen microsensors (Revsbech 1989) mounted in a motorised micromanipulator (Märtzhäuser and Unisense). The microsensors had tip diameters of 10 to 130 μm , a stirring sensitivity of <1 to 2% and a 90% response time of ~0.4 s. The microsensors were connected to a picoampere meter (PA2000, Unisense) and the mea-

suring signals were recorded on a PC with either a custom-made computer data-acquisition system ('Lab-View', National Instruments) or a commercial data acquisition system ('Profix', Unisense). Both systems also controlled the motorised micromanipulator. Linear calibration of oxygen microsensors was done from electrode readings in air-saturated water and in the anoxic part of the sediment. The oxygen concentration in air-saturated water of known salinity and temperature was taken from tables available from Unisense at www.unisense.com/support/pdf/gas_tables.pdf.

Experimental set-up for microsensor measurements. The roots selected for measurements were washed free of adhering sediment particles, while carefully avoiding disruption of the root cap, and were then placed horizontally in the sediment. The microsensor tip was positioned at the root surface while observed under a dissecting microscope. By this method we could also determine exactly where on the roots the profiles were recorded in relation to the root tip. After positioning of the microsensor, the roots were gently covered with sediment again and the microsensor was either removed from the root surface by use of the motorised micromanipulator (10 to 12 μm sized microsensor tips) or left at the surface of the roots (10 and 130 μm sized microsensor tips). After the root had been covered with sediment, repeated microsensor measurements showed that steady state profiles were established within 30 min in darkness and at irradiances $>230 \mu\text{mol photons m}^{-2} \text{s}^{-1}$, and within ~ 1 h at lower irradiances.

Oxygen measurements on roots and rhizomes from different plants. Oxygen concentrations on the root surface were measured with a robust microelectrode (130 μm tip diameter) at distances of 0, 1, 2, 3, 4, 5, 6, 7, 14, and 21 mm from the root tip on roots of 4 different plants exposed to an irradiance of $467 \mu\text{mol photons m}^{-2} \text{s}^{-1}$. Before every new measurement, the electrode was positioned at the root surface by the method described above. Radial oxygen concentration profiles around roots were measured with a thinner microelectrode (tip size 10 to 12 μm) on 2 different plants at distances of 0, 1, 2, 3, 4, 5, and 6 mm from the root tip.

Oxygen measurements at different light intensities. To investigate the O_2 leakage as a function of plant photosynthesis, the microsensor tip was positioned 2 mm behind the root tip, i.e. within the region exhibiting the highest radial oxygen loss. Surface concentrations and oxygen profiles were measured on 4 plants in darkness and at 3 to 8 different irradiances (0 to $793 \mu\text{mol photons m}^{-2} \text{s}^{-1}$). After positioning the oxygen microsensor, plants were left in darkness for 30 min before the first profiles or surface concentrations were measured.

Flux calculations. Assuming that the measured radial oxygen profiles represented profiles from separate parts of a perfect cylinder with a homogeneous oxygen loss, we calculated radial oxygen fluxes, $J(r)$ ($\text{nmol O}_2 \text{ cm}^{-2} \text{ h}^{-1}$), from the root by a cylindrical version of Fick's first law of diffusion (Steen-Knudsen 2002):

$$J(r)_{\text{root}} = \phi D_s (C_1 - C_2) / r \ln(r_1/r_2) \quad (1)$$

where ϕ is the porosity, D_s is the diffusion coefficient of oxygen in the sediment, r is the radius of the root and C_1 and C_2 represent the measured oxygen concentrations at r_1 and r_2 , i.e. the radius of an inner and outer cylinder shell, respectively (corresponding to distances from the root centre).

The porosity, ϕ , was determined to be 0.4 from the weight loss of 4×10 ml of water-saturated sediment after drying to constant weight in a 105°C oven. D_s was calculated to be $8.5 \times 10^{-6} \text{ cm}^2 \text{ s}^{-1}$ from the equation $D_s = D_0 / [1 + n(1 - \phi)]$ using a value of $n = 2$ for sandy sediments (Iversen & Jørgensen 1992). The molecular diffusion coefficient of oxygen in water, D_0 , at experimental temperature and salinity was taken from tables available from Unisense A/S (www.unisense.com/support/pdf/gas_tables.pdf).

The total oxygen export M ($\text{nmol O}_2 \text{ h}^{-1}$) from 1 root of the first actively growing root bundle was calculated as $M = \int J(r)_{\text{cylinder}} d(z)$, where z is the distance from the root tip apex (see Table 1). The radial oxygen loss from >6 mm from the root tip and up to the rhizome was assumed to be homogeneous and the root was assumed to be 60 mm long. The integral was approximated by summation and calculated using the following equation (Steen-Knudsen 2002):

$$M = \sum -2\pi \Delta z \phi D_s \times (C_1 - C_2) / \ln(r_1/r_2) \quad (2)$$

where Δz is the distance along the root axis.

The equations for calculating oxygen fluxes, ROL, and total oxygen export, $M(r)$, are sensitive to the exact value of the radius of the root, especially for values close to the root surface. Occasionally, we struck the root just before the surface measuring point, and at distances further away from the root surface the consumption of oxygen changed compared to distances closer to the root surface. We therefore determined $\Delta C / \ln(r_1/r_2)$ for each profile by plotting C_n against $\ln(r_n)$ and performed a linear regression of the \ln -transformed data using measuring points at distances 0.005 to 0.025 cm away from the root surface.

Planar optode measurements. The 2-dimensional oxygen distribution around *Zostera marina* roots was mapped with a 20 μm thick ruthenium-type planar oxygen optode (Glud et al. 1996), covered with a 40 μm thick insulation of black silicone. The response time of the planar optode was ~ 10 s (Klimant et al. 1995, Glud

et al. 1996). The planar optode was used together with a fluorescence-lifetime imaging system (Holst et al. 1998), here only used in the fluorescence-intensity mode. Calibration of the optode was made in N_2 - and O_2 -saturated water both before and after measurements. Further details on image-recording and calibration calculations can be found in Glud et al. (1996) and Holst et al. (1998).

The planar optode was fixed on the side of a 5 l aquarium, carefully avoiding formation of air bubbles between the glass and the optode, and 8 thin cotton threads were loosely fixed horizontally with tape on the planar optode ~5 mm apart. Plant roots were placed vertically between the threads and the planar optode, and the roots were gently pressed against the optode by tightening the cotton threads. The roots and rhizome were then covered with sediment ensuring that the roots placed in the 'thread system' remained in place. Image-recording was done after 30 min of pre-incubation.

Root histology. The roots were cut into 1.5 to 2 mm pieces, fixed in 3% glutaraldehyde in 0.1 M phosphate buffer, pH 7.0, dehydrated in methoxyethanol, ethanol, propanol and butanol, and embedded in glycolmethacrylate. We cut 3 μ m thick sections on a microtome (LKB Historange) with glass knives made on LKB Knifemaker Type 7801B, and transferred them to microscope glass slides in drops of distilled water. The sections were stained with Toluidine Blue O, examined with light microscopy (Reichert Jung Polyvar) and photographed with a CCD-video camera (Evolution LC) connected to a PC and processed with the 'Image Pro Plus' software package.

RESULTS

Root growth patterns

The roots of *Zostera marina* grew approximately 5 mm d⁻¹, with a new root bundle developing every 7 to 10 d (Fig. 1A). The roots grew to a length of 45 to 60 mm and had a diameter of ~0.3 mm. Preliminary histological studies showed that young roots of *Z. marina* are characterised by numerous intercellular spaces present in longitudinal rows close to the apical meristem of the root (Fig. 1B) and by the presence of a 3 to 4 mm-long root cap (data not shown).

Oxygen concentrations along root surface

Although the oxygen concentrations at the surface of the roots differed substantially among different plants, a distinct pattern was obvious (Figs. 2 & 3). In saturating light (>400 μ mol photons m⁻² s⁻¹), the oxygen concentration was 5 to 33% of air saturation at the root apex, increasing to a maximum of 19 to 80% 1 to 2 mm behind the apex, decreasing to ~0 to 5% of air saturation 3 to 6 mm away from the root tip, and then reaching levels of zero oxygen on the more mature parts of the root (data only shown for 2 plants in Fig. 2).

Oxygen measurements at different irradiances

Surface concentrations were significantly different between dark and light incubations (Fig. 4A). The

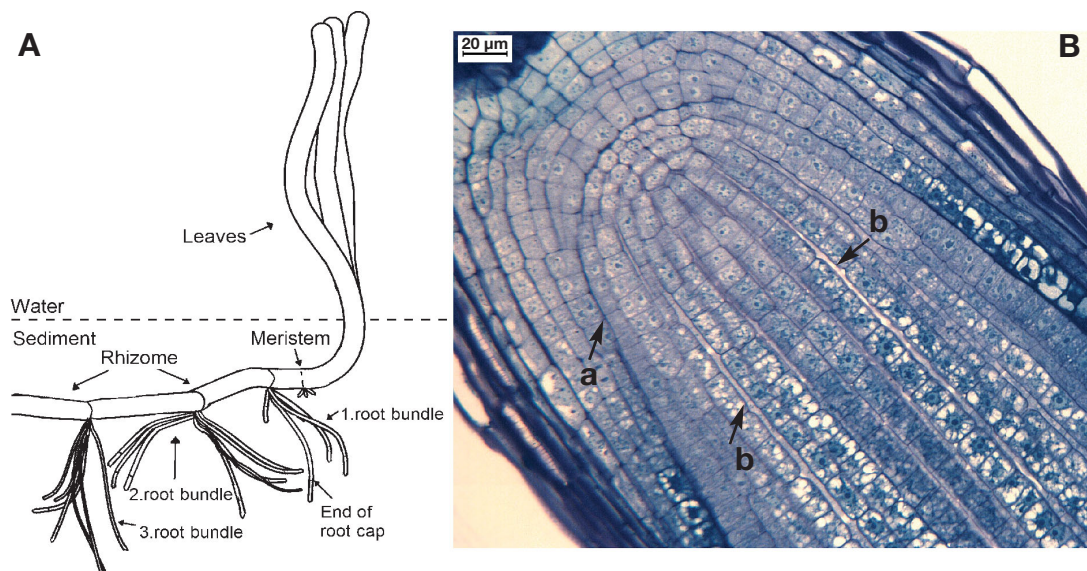


Fig. 1. *Zostera marina*. (A) Root system (partly redrawn from Pedersen et al. 2004); (B) longitudinal section of root tip embedded in glycolmethacrylate, stained with Toluidine Blue O and examined with light microscopy. Arrows indicate border between root cap and root proper (a) and intercellular spaces (b)

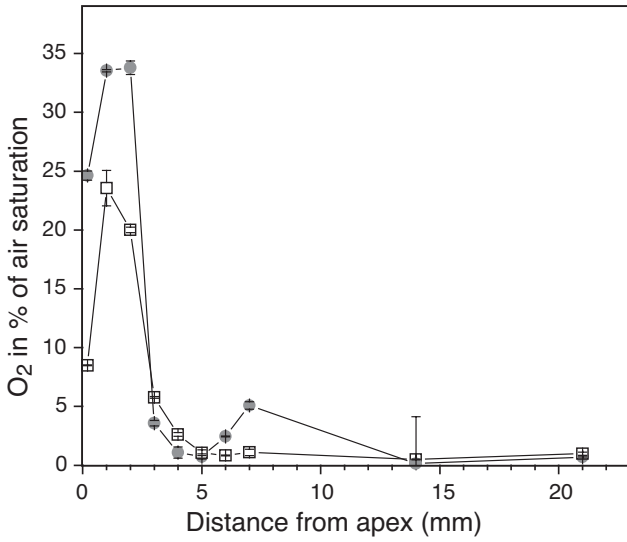


Fig. 2. *Zostera marina*. Oxygen concentration at root surface measured at various distances from root apex of (□) 45 mm and (●) 25 mm long roots. Data are means ± SD of 2 to 3 measurements taken 5 min apart

oxygen level at the root surface and the ROL was stimulated by light until it reached saturation at irradiances >400 μmol photons m⁻² s⁻¹. The oxygen concentration at the root surface changed from 7 to 30% air saturation in darkness to 30 to 80% air saturation at the highest experimental irradiances (data only shown for 2 plants in Fig. 4). ROL varied from 16.2 nmol O₂ cm⁻² h⁻¹ in darkness to 21.6, 28.8 and 36.0 nmol O₂ cm⁻² h⁻¹ at irradiances of 25, 111 and 467 μmol photons m⁻² s⁻¹,

Table 1. *Zostera marina*. Radial oxygen loss, $J(r)$, and the total oxygen export, $M(r)$, calculated at different distances from the root apex for 2 roots of the first actively growing root bundle of 2 different plants. Distance: distance behind root tip; Root-zone distance: distance of 1 mm 'zones' away from root tip; -: not determined

Distance (mm)	$J(r)$ (nmol O ₂ cm ⁻² h ⁻¹)		Root-zone distance (mm)	$M(r)$ (nmol O ₂ h ⁻¹)	
	Root 1	Root 2		Root 1	Root 2
0.2	59.4	67.6	-0.5-0.5	0.56	0.64
1	92.7	69.0	0.5-1.5	0.87	0.65
2	58.0	95.5	1.5-2.5	0.55	0.90
3	12.3	73.4	2.5-3.5	0.12	0.69
4	11.4	71.6	3.5-4.5	0.11	0.67
5	19.0	13.8	4.5-5.5	0.18	0.13
6-45	6.9	5.8	5.5-45	2.58	2.17
6-60	-	-	5.5-60	3.56	2.99

respectively. Plants with the highest surface concentrations and ROL in the light also exhibited the highest surface concentrations and ROL in darkness.

Oxygen profiles and total flux from *Zostera marina* roots

Oxygen penetrated 0 to 1.0 mm from the root surface into the sediment, depending on irradiance and distance behind the root tip (Figs. 3B & 4B). The ROL varied from 5.8 nmol O₂ cm⁻² h⁻¹ 6 mm behind the root tip to 95.5 nmol O₂ cm⁻² h⁻¹ 1 to 2 mm behind the root tip (Table 1, Fig. 3), and showed a linear relationship with the corresponding surface concentrations (data not shown). The total oxygen export in saturating light was calculated

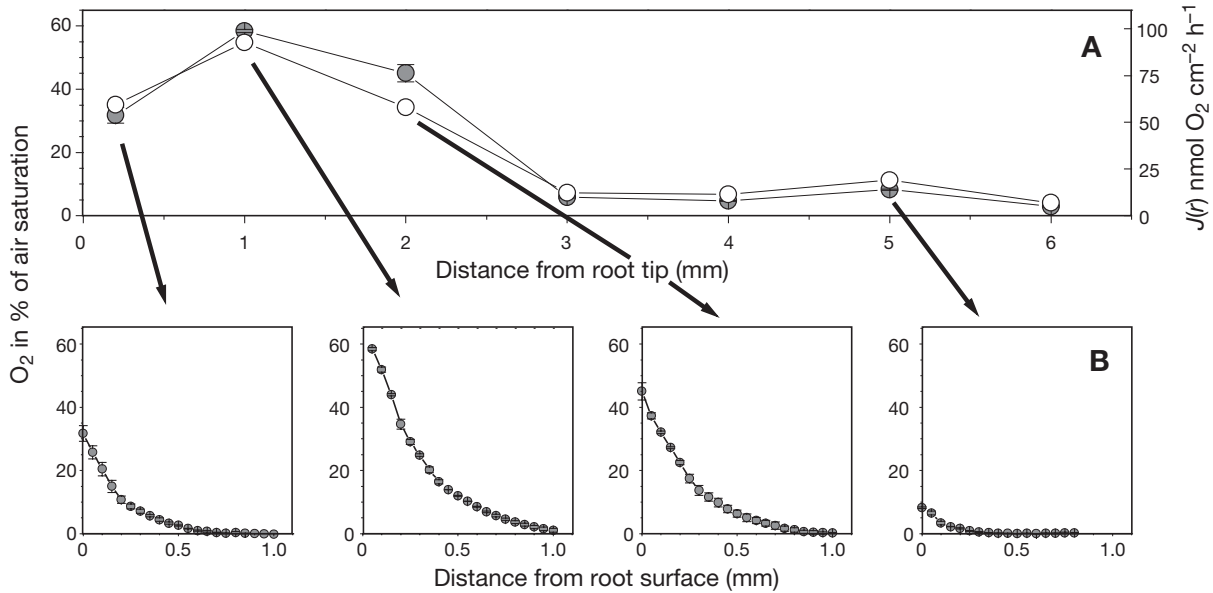


Fig. 3. *Zostera marina*. (A) Oxygen concentration at root surface data are means ± SD of 3 measurements taken 5 min apart (●) and (○) radial oxygen fluxes, both as a function of distance from root tip; (B) 4 examples of corresponding radial oxygen profiles (means ± SD of 2 to 3 profiles taken 10 min apart)

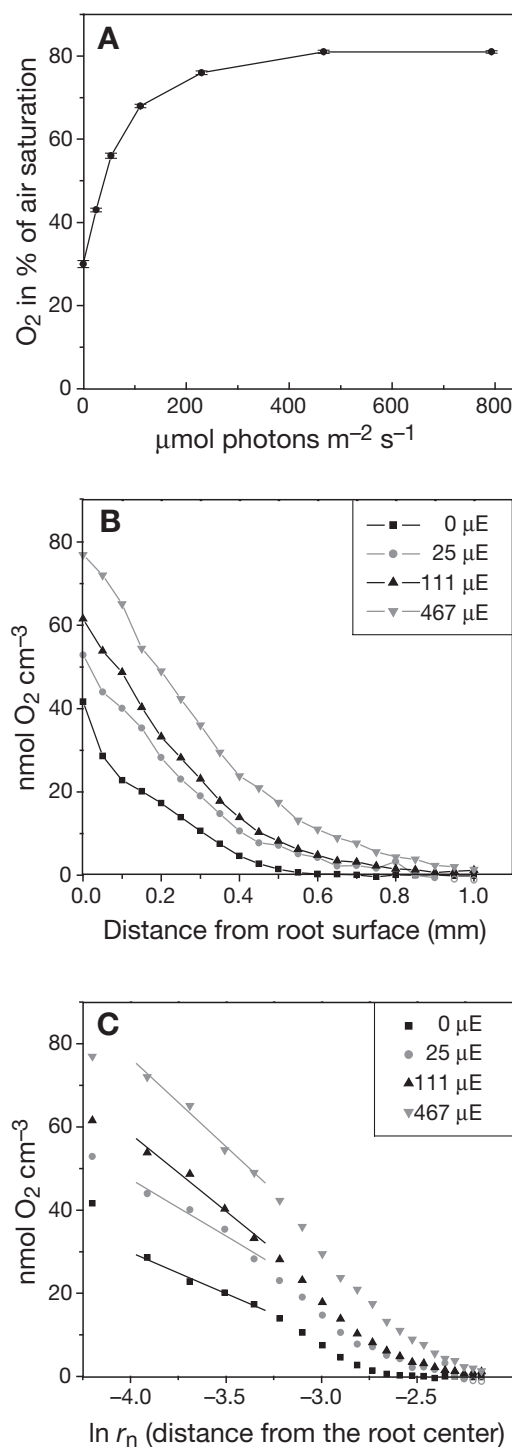


Fig. 4. *Zostera marina*. (A) Oxygen concentration at root surface measured 2 mm behind apex as a function of irradiance; data are means \pm SD of 3 measurements taken 5 to 10 min apart. (B,C) Steady state radial oxygen profiles at different irradiances measured on another root 2 mm behind apex, showing oxygen concentration as a function of (B) distance from root surface and (C) distance from root centre, $\ln(r)$. Lines indicate slopes used for calculations of flux $J(r)$ and mass transport $M(r)$

from the values in Table 1 as 6.0 and 6.7 nmol O₂ h⁻¹ root⁻¹ for 2 different plant roots from the first actively growing root bundle of 2 different plants, assuming a root length of 60 mm. The oxygen loss in the 1 mm zone of the root cap exhibiting the highest ROL was 13 to 16 times higher than the loss from a 1 mm root-zone at a distance >6 mm away from the root tip, and the root tip region 0 to 3.5 mm from the root apex contributed 35 to 43% of the total oxygen loss from 1 root.

In this study we have only presented detailed studies on the ROL from roots of the youngest actively growing root bundle. Point measurements made on other parts of the plant in the sediment showed that ROL also occurs from the meristematic region of the rhizome (see Fig. 1), but at a much smaller magnitude than the ROL from the root tips of the first actively growing root bundle. ROL from the second root bundle showed a variable ROL in the 0 to 3 mm root tip region, with ROL varying from almost zero to the same values measured for the root tip region of the first root bundle. No ROL was found in higher regions of the second root bundle, and we did not see any measurable ROL for regions of the older third root bundle (data not shown).

Planar optodes

The 2-dimensional oxygen distribution around the roots of a *Zostera marina* plant is presented in Fig. 5. Like the microsensor data, the planar optode data showed a local oxygen leakage from the root tip region. However, with the planar optode the total width of the oxygenated zone, including the root, extended up to 5 mm, whereas the total width of the oxygenated zone measured with the microsensors was maximally 2.3 mm including the root (Fig. 3B). For the more mature parts of the roots, we did not see any oxygen leakage occurring when measuring with the planar optodes.

DISCUSSION

Microelectrodes versus planar optodes

Differences in ROL along the roots of plants have previously been studied with plants rooted in agar (e.g. Armstrong 1971, Connell et al. 1999), while knowledge about the distribution of oxygen in the natural rhizosphere of plants is still very limited. By the use of microelectrodes we were able to determine the distribution of oxygen and the associated ROL at high spatial resolution along the axis of *Zostera marina* roots measured in their natural substratum. The manipulation of the sediment prior to the measurements might, however, have affected the redox conditions of the sedi-

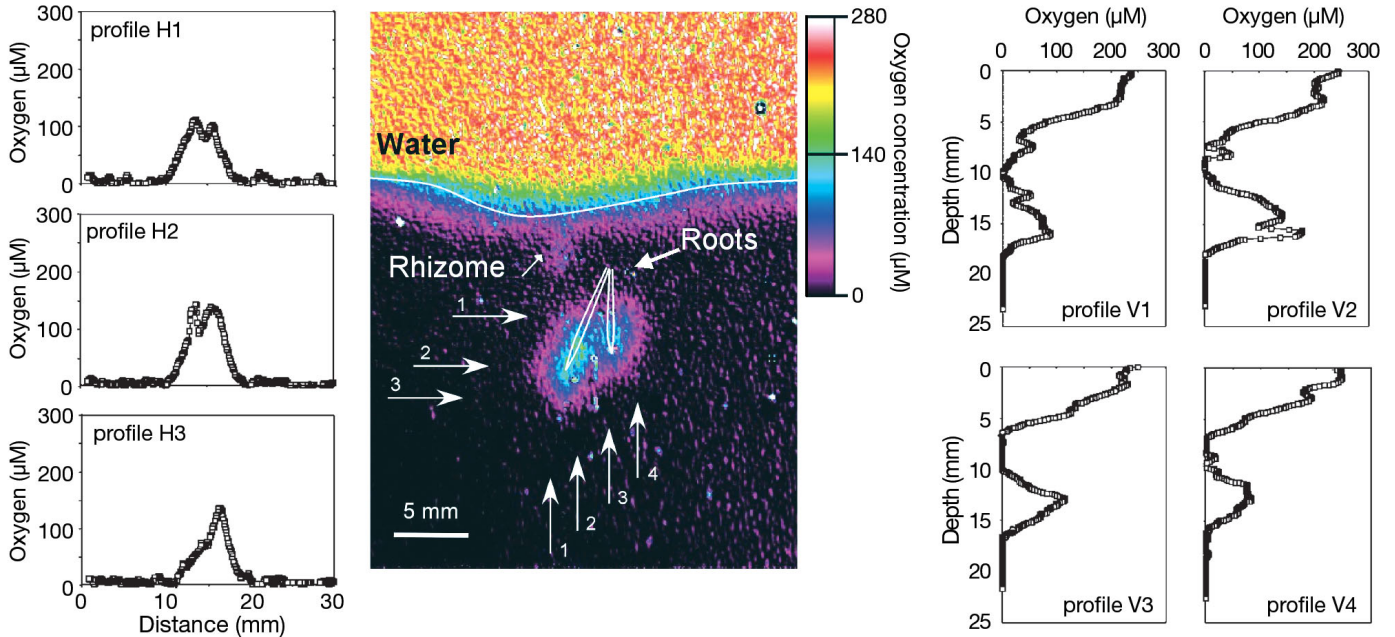


Fig. 5. *Zostera marina*. Oxygen distribution and profiles. Central panel shows 2-dimensional oxygen distribution around roots. White lines show approximate positions of roots and sediment surface; arrows indicate locations of extracted horizontal (H) and vertical (V) oxygen profiles shown in left and right graphs, respectively

ment, especially around the more mature parts of the roots, where a destruction of an eventual biofilm around the roots could have affected microbial consumption substantially. We do not, however, expect the oxygenated zone on the more distal parts of the roots to have been highly overrated. Measurements 3.5 mm behind the root tip revealed that the width of the oxygenated zone measured in the light only decreased about 50 μm after 10 h in darkness, and the width of the oxygenated zone during darkness remained constant (data not shown).

A significant experimental problem was caused by the fact that the roots started to grow again during the up to 8 h long experiments with different irradiances. Consequently, the profiles or surface concentrations measured under the higher irradiances might have been made in a section of the root exhibiting a different ROL compared to the measurements during the lower irradiances. With the pronounced differences in ROL we found along the root (Figs. 2 & 3), this may have caused some artefacts. Our experimental cycles were therefore time limited by root growth. This emphasises the advantage of methods such as the use of planar optodes, by which the 2-dimensional oxygen distribution around roots can be followed rapidly during root growth.

By the use of planar optodes we could map the oxygen distribution along a larger area of the roots, making measurements on the spatial oxygen distribution in the rhizosphere and the associated ROL less

time consuming. We did not observe any oxygen loss from the more mature parts of the roots, and we speculate that these differences may have been caused by the presence of root hairs, pushing the plant root away from the planar surface at a distance where the small oxygen concentrations of the root surface measured by the microelectrodes were not detected by the planar optode. A useful and quick picture of the oxygen distribution around several roots at the same time might however still be made with the planar optodes, since we found that up to 43% of the total oxygen loss was occurring in the smooth root tip region.

Another difference in the results obtained by the planar optode compared with microsensor data was the extension of the oxygenated zone. The planar optode, along with the glass wall behind it, represents a barrier for oxygen, causing a 2-dimensional smearing of the oxygenated zone around the root. Furthermore, the optode matrix itself and the black silicone coating may facilitate lateral oxygen diffusion, contributing to the smearing effect; preliminary modelling of this effect showed, however, no significant effect of the silicone layer. The use of the thread system might also have increased this smearing, since the root diameter could have been extended when the roots were pressed against the planar surface. More combined studies with planar optodes and microelectrodes are needed to assess and evaluate potential caveats of the applied approaches, and optimised set-ups for planar measuring techniques is required—such work is in progress.

Oxygen loss from *Zostera marina* and its impact on sediment biogeochemistry

The oxygen concentrations, oxygen fluxes and oxygen penetration depths varied substantially within a few millimetres along the roots of any one plant (Figs. 2 & 3). Light (Fig. 4A,B) and possibly also other physical conditions like temperature (Greve et al. 2003) and water flow around the plant leaves (T. Binzer pers. comm.) have a high impact on the ROL from the roots. Our data indicate that the root tip exhibiting the highest ROL will only generate an oxic microzone for <24 h during root growth. Recent planar optode studies have confirmed this ephemeral nature of the oxic microzonation in the rhizosphere of *Zostera marina* (M. Frederiksen & R. N. Glud unpubl. data). Observations on frozen *Zostera marina*-containing sediment revealed that this short time period is apparently enough to induce a ~0.5 mm wide oxidised but anaerobic microzone around the more mature parts of the young roots of the first actively growing root bundle.

The radial oxygen loss from a root is closely related to the distance from the apical meristem of the root, and a rough estimation of the total oxygen export from *Zostera marina* roots can be calculated as $0.1 \mu\text{mol O}_2 \text{ h}^{-1} \text{ shoot}^{-1}$, assuming a total oxygen loss of $6.7 \text{ nmol O}_2 \text{ h}^{-1} \text{ root}^{-1}$ (Table 1) and an equal amount of oxygen loss from 16 roots, each 6 cm long, i.e. the 2 youngest root bundles in this study. From flux calculations on steady-state oxygen profiles measured in darkness (data not shown), the diffusive oxygen uptake (DOU) across the primary sediment–water interface was calculated as $1.6 \text{ mmol O}_2 \text{ m}^{-2} \text{ h}^{-1}$.

The mean shoot density within 29 eelgrass beds in the temperate regions of the northern hemisphere has been estimated at $905 \text{ shoots m}^{-2}$ in the summer, varying from 257 to $2193 \text{ shoots m}^{-2}$ (Olesen & Sand-Jensen 1994). On the basis of these data along with our estimation of the oxygen export per plant shoot, the average total plant mediated oxygen export in *Zostera marina*-inhabited sediments can be calculated as $0.09 \text{ mmol O}_2 \text{ m}^{-2} \text{ h}^{-1}$ (6% of DOU in the present study) in saturating light, with variations of 0.03 to $0.22 \text{ mmol O}_2 \text{ m}^{-2} \text{ h}^{-1}$ (2 to 14% of DOU in the present study). In comparison, a coverage of benthic diatoms exhibits a net oxygen production of 8 to $13.5 \text{ mmol O}_2 \text{ m}^{-2} \text{ h}^{-1}$, and causes an effective transport of oxygen down into the deeper sediment of 2.8 to $4.7 \text{ mmol O}_2 \text{ m}^{-2} \text{ h}^{-1}$ (Fenchel & Glud 2000) indicating that oxygen leakage from *Z. marina* roots makes but a minor contribution to the total oxygen content of the sediments. Nevertheless, a dense bed of *Z. marina*, with sediment characteristics similar to those in our experiment, can potentially increase the total oxygen transport to the sediment by up to 14% during the daytime without

ROL from the rhizomes. The relatively small oxygen export is largely due to the fact that oxygen leakage from *Z. marina* only occurs over a small surface area of the roots. Previous estimations of the total oxygen loss have been made for *Cymodocea rotundata* inhabited sediments (Pedersen et al. 1998). Based on a few point measurements, the total oxygen loss was calculated to correspond to the DOU at the sediment–water interface. This might however be either an over- or under-estimation, if *C. rotundata* possesses a barrier to ROL as has now been shown for both *Halophila ovalis* (Connell et al. 1999) and *Z. marina* (this study). If we had based our estimation on an approach similar as to that of Pedersen et al. (1998), the total transport of oxygen could, on basis of the above mentioned assumptions, have varied from 0 to $1.9 \text{ mmol O}_2 \text{ m}^{-2} \text{ h}^{-1}$ (119% of the DOU) in a high density eelgrass bed.

Our estimation has been made on the basis of a detailed investigation of the ROL from *Zostera marina* roots, but morphological characteristics such as root numbers, thickness of roots and development of lacunae differ strongly between individual plants (Penhale & Wetzel 1983). Furthermore, our measurements were made on plants growing in separate pots, which might have induced a stronger barrier to ROL than when plants are growing in clusters under well oxygenated growth conditions. Anaerobic conditions as well as phytotoxins have been shown to induce a stronger barrier to ROL (Colmer et al. 1998, Armstrong & Armstrong 2001). When *Z. marina* grows in a dense seagrass bed under favourable conditions in relation to internal oxygen concentrations, new roots might penetrate sediment already oxidised, be less subject to phytotoxin effects, and thus possibly not have a barrier to ROL as close to the root tips as in our experiments. This potential cluster effect would be similar to the increased oxygen leakage from plants having fine laterals such as *Phragmites australis*, in which the lateral roots causes considerable oxygenation of the sediment (Armstrong & Armstrong 2001). Our data may therefore be more representative for *Z. marina* plants growing in clusters under poor conditions in relation to internal oxygen concentrations and increased exposure to phytotoxins, than for plants growing under more favourable conditions. More measurements on the spatial distribution of ROL (e.g. by *in situ* application of microsensors and planar optodes, Glud et al. 2001), as well as studies on root biomass dynamics are therefore required to assess the potential plant mediated oxygen release at individual sites.

The local oxygen flux from the root tips of *Zostera marina* was in the same range (up to 60%) as the oxygen flux at the primary sediment–water interface. The oxygen loss from the root tips of *Z. marina* is thus high enough to significantly affect the zonation of biogeo-

chemical processes in the immediate rhizosphere of the roots, as previously inferred from porewater analysis and vertical profiling of Fe^{2+} and H_2S (Herbert & Morse 2003). This, along with the spatio-temporal dynamics of ROL in relation to light and root morphology found in this and other studies of aquatic plants, complicates the interpretation of biogeochemical processes from coarse analysis of core samples in plant inhabited sediments and wetland soils. Furthermore, separating the roots from the oxygen providing leaves or conducting experiments in darkness, as was done in some studies, will affect the redox conditions in the rhizosphere significantly and may have severe effects on the rates measured.

Barrier to ROL and its effect on *Zostera marina*

Our morphological studies of the roots of *Zostera marina* showed that intercellular spaces were present close to the apical meristem of the roots, indicating a very effective gas transport system from the leaves to the roots. Furthermore, our oxygen microsensor data showed the presence of a strong barrier to ROL. The barrier to ROL in *Z. marina* occurred within the first 5 mm from the root tip, which is the closest barrier to ROL in relation to distance from root tip reported so far. Previous studies have reported a barrier to ROL within a few centimetres from the root tip (e.g. Armstrong 1971 [*Oryza* spp.]), Connell et al. 1999 [*Halophila ovalis*]). The maximum ROL from *H. ovalis* varied between 59.4 and 185.0 $\text{nmol O}_2 \text{ cm}^{-2} \text{ h}^{-1}$ (Connell et al. 1999), while we found the maximum ROL from *Z. marina* roots to be somewhat lower, varying between 92.7 and 95.5 $\text{nmol O}_2 \text{ cm}^{-2} \text{ h}^{-1}$). The presence of a barrier to ROL so close the root tip might suggest that *Z. marina* is better adapted to life in reduced sediments than *H. ovalis*, but could also be a simple response to the differences in the 2 root systems due to a longer transport path of oxygen from the leaves to the older root tips and more roots per root bundle in *Z. marina*.

If a barrier to ROL were not present in the extensive root system of *Zostera marina*, several root tips could possibly not be oxygenated and ROL would lead to low intra-plant oxygen concentrations even under favourable conditions. Pedersen et al. (2004) suggested that sulphide intrusion is prevented at high internal oxygen concentrations by a complete re-oxidation of sulphide in the sediment immediately surrounding the roots. Our results show, however, that such a microshield of oxygen cannot be expected in the more mature parts of the roots even with plants kept in saturating light. The barrier to ROL could function as a barrier towards toxic gaseous substances such as H_2S , but sulphide re-oxidation could also occur in the outermost cell layers

of the roots rather than in the sediment. The latter possibility awaits a detailed analysis of the distribution of oxidised sulphur compounds such as S^0 in the roots as well as detailed sulphide microsensor measurements in the rhizosphere of *Z. marina*.

What causes the barrier to ROL?

It has been suggested that a barrier to ROL is caused by the presence of suberised lamellae in the exodermis of plant roots (e.g. Enstone et al. 2003). Barnabas (1996) found Casparian band-like structures composed of suberin in the hypodermis of the roots of all investigated marine angiosperms, including *Zostera marina*, and suggested that these features might protect the plant from toxic substances in the sediment. An additional reason for the barrier to ROL along the roots of *Z. marina* could be the growth of bacteria on the immediate surface of the roots and within the outermost cell layers of the roots as the roots mature. Bacteria have been shown to be present within the roots of marine angiosperms (Kuo 1993), and 2 sulphate-reducing bacteria (Nielsen et al. 1999, Finster et al. 2001) have been isolated from surface-sterilised roots of *Z. marina*.

If the barrier to ROL is caused mainly by the presence of plant specific substances inducing low gas permeability, it is likely that the barrier to ROL also provides a protection against toxic gases like H_2S . However, the root tip of growing roots does not have this feature, and is therefore dependent on oxygen release to detoxify H_2S . Our results show that a microshield of oxygen surrounds the root tips even in darkness; at least when the plant is kept in stirred, aerated water.

If the barrier to ROL is partly caused by bacterial colonisation this can have severe effects on the root system, e.g. under low light conditions. Kuo (1993) suggested that bacteria can break down the Casparian band like structures, and if bacteria colonise the outermost cell layers of the roots they may break down plant tissue, barriers to gas transport in oxygen depleted roots facilitating an inward diffusion of H_2S . Little is known about the distribution of microorganisms in the rhizosphere of aquatic plants, and more microscale studies on this subject are needed to provide an insight into these potentially important plant–bacteria interactions.

Acknowledgements. We thank A. Glud and L. F. Rickelt for construction of the microelectrodes and planar optodes used in this study. T. Binzer and R. Thar are thanked for practical help and advice and J. Borum for comments during the preparation of the manuscript. The study was funded by the Danish Natural Science Research Council and the European Commission (contract numbers QLK-CT-2002-01938, EVK3-CT2001-00210, EVK-CT2002-0076).

LITERATURE CITED

- Armstrong J, Armstrong W (2001) Rice and *Phragmites*: effects of organic acids on growth, root permeability, and radial oxygen loss to the rhizosphere. *Am J Bot* 88:1359–1370
- Armstrong W (1971) Radial oxygen losses from intact rice roots as affected by distance from the apex, respiration and water logging. *Physiol Plant* 25:192–197
- Armstrong W (1979) Aeration in higher plants. Academic Press, London
- Armstrong W, Cousins D, Armstrong J, Turner DW, Beckett PM (2000) Oxygen distribution in wetland plant roots and permeability barriers to gas-exchange with the rhizosphere: a microelectrode and modelling study with *Phragmites australis*. *Ann Bot Fenn* 86:687–703
- Barnabas AD (1996) Casparian band-like structures in the root hypodermis of some aquatic angiosperms. *Aquat Bot* 55:217–225
- Blaabjerg V, Mouritsen KN, Finster K (1998) Diel cycles of sulphate reduction rates in sediments of a *Zostera marina* bed (Denmark). *Aquat Microb Ecol* 15:97–102
- Caffrey JM, Kemp WM (1991) Seasonal and spatial patterns of oxygen production, respiration and root-rhizome release in *Potamogeton perfoliatus* L. and *Zostera marina* L. *Aquat Bot* 40:109–128
- Christensen PB, Revsbech NP, Sand-Jensen K (1994) Microsensor analysis of oxygen in the rhizosphere of the aquatic macrophyte *Littorella uniflora* (L.) Ascherson. *Plant Physiol* 105:847–852
- Colmer TD (2003) Long-distance transport of gases in plants: a perspective on internal aeration and radial oxygen loss from roots. *Plant Cell Environ* 26:17–36
- Colmer TD, Gibberd MR, Wiengweera A, Thin TK (1998) The barrier to radial oxygen loss from roots of rice (*Oryza sativa* L.) is induced by growth in stagnant solution. *J Exp Bot* 49:1431–1436
- Connell EL, Colmer TD, Walker DI (1999) Radial oxygen loss from intact roots of *Halophila ovalis* as a function of distance behind the root tip and shoot illumination. *Aquat Bot* 63:219–228
- Enstone DE, Peterson CA, Ma F (2003) Root endodermis and exodermis: structure, function, and responses to the environment. *J Plant Growth Regul* 21:335–351
- Fenchel T, Glud RN (2000) Benthic primary production and O₂-CO₂ dynamics in a shallow-water sediment: spatial and temporal heterogeneity. *Ophelia* 53:159–171
- Finster K, Thomsen TR, Ramsing NB (2001) *Desulfomusa hansenii* gen. nov., sp. nov., a novel marine propionate-degrading, sulfate-reducing bacterium isolated from *Zostera marina* roots. *Int J Syst Bacteriol* 51:2055–2061
- Glud RN, Ramsing NB, Gundersen JK, Klimant I (1996) Planar optodes, a new tool for fine scale measurements of 2 dimensional O₂ distribution in benthic communities. *Mar Ecol Prog Ser* 140:217–226
- Glud RN, Kühl M, Kohls O, Ramsing NB (1999) Heterogeneity of oxygen production and consumption in a photosynthetic microbial mat as studied by planar optodes. *J Phycol* 35:270–279
- Glud RN, Tengberg A, Kühl M, Hall POJ, Klimant I, Holst G (2001) An *in situ* instrument for planar O₂ optode measurements at benthic interfaces. *Limnol Oceanogr* 46:2073–2080
- Greve TM, Borum J, Pedersen O (2003) Meristematic oxygen variability in eelgrass (*Zostera marina*). *Limnol Oceanogr* 48:210–216
- Herbert AB, Morse JW (2003) Microscale effects of light on H₂S and Fe²⁺ in vegetated (*Zostera marina*) sediments. *Mar Chem* 81:1–9
- Holmer M, Nielsen SL (1997) Sediment sulfur dynamics related to biomass-density patterns in *Zostera marina* (eelgrass) beds. *Mar Ecol Prog Ser* 146:163–171
- Holst G, Kohls O, Klimant I, König B, Kühl M, Richter T (1998) A modular luminescence lifetime imaging system for mapping oxygen distribution in biological samples. *Sens Act B* 51:163–170
- Iversen N, Jørgensen BB (1992) Diffusion coefficients of sulfate and methane in marine sediments: influence of porosity. *Geochim Cosmochim Acta* 57:571–578
- Jørgensen BB (1982) Mineralization of organic matter in the sea bed—the role of sulfate reduction. *Nature* 296:643–645
- Klimant I, Meyer V, Kühl M (1995) Fiber-optic oxygen microsensors, a new tool in aquatic biology. *Limnol Oceanogr* 40:1159–1165
- Kuo J (1993) Root anatomy and rhizosphere ultrastructure in tropical seagrasses. *Aust J Mar Freshw Res* 44:75–84
- Nielsen JT, Liesack W, Finster K (1999) *Desulfovibrio zosterae* sp. nov., a new sulfate reducer isolated from surface-sterilized roots of the seagrass *Zostera marina*. *Int J Syst Bacteriol* 49:859–865
- Nordi G (2004) Microniches in marine sediments: effect of sedimented aggregates and plant root oxygen leakage. MS thesis, University of Copenhagen, Helsingør
- Olesen B, Sand-Jensen K (1994) Biomass-density patterns in the temperate seagrass *Zostera marina*. *Mar Ecol Prog Ser* 109:283–291
- Pedersen O, Borum J, Duarte CM, Fortes MD (1998) Oxygen dynamics in the rhizosphere of *Cymodocea rotundata*. *Mar Ecol Prog Ser* 169:283–288
- Pedersen O, Binzer T, Borum J (2004) Sulphide intrusion in eelgrass (*Zostera marina* L.). *Plant Cell Environ* 27:595–602
- Penhale PA, Wetzel RG (1983) Structural and functional adaptations of eelgrass (*Zostera marina* L.) to the anaerobic sediment environment. *Can J Bot* 61:1421–1428
- Revsbech NP (1989) An oxygen microelectrode with a guard cathode. *Limnol Oceanogr* 34:474–478
- Revsbech NP, Pedersen O, Reichardt W, Briones A (1999) Microsensor analysis of oxygen and pH in the rice rhizosphere under field and laboratory conditions. *Biol Fertil Soils* 29:379–385
- Sand-Jensen K, Prah C, Stockholm H (1982) Oxygen release from roots of submerged aquatic macrophytes. *Oikos* 38:349–354
- Steen-Knudsen O (2002) Biological membranes. Cambridge University Press, Cambridge
- Terrados J, Duarte CM, Kamp-Nielsen L, Agawin NSR and 6 others (1999) Are seagrass growth and survival constrained by the reducing conditions of the sediment? *Aquat Bot* 65:175–197
- Visser EJW, Colmer TD, Blom CWPM, Voesenek LACJ (2000) Changes in growth, porosity, and radial oxygen loss from adventitious roots of selected mono- and dicotyledonous wetland species with contrasting types of aerenchyma. *Plant Cell Environ* 23:1237–1245
- Welsh DT, Bartoli M, Nizzoli D, Castaldelli G, Riou SA, Viaroli P (2000) Denitrification, nitrogen fixation, community primary productivity and inorganic-N and oxygen fluxes in an intertidal *Zostera noltii* meadow. *Mar Ecol Prog Ser* 208:65–77